ISSN : 0974 - 7486 Volume 14 Issue 5

Materials Science

An Indian Journal

Full Paper

MSAIJ, 14(5), 2016 [184-190]

Influence of the carbon content and of a plastic deformation on the corrosion behaviour of cast carbon steels. Part 1: Microstructure and compression properties

Manale Belhabib[1], Patrice Berthod[1,2]*

[1]Faculty of Sciences and Technologies, University of Lorraine, B.P. 70239, 54506 Vandoeuvre-lès-Nancy, (FRANCE)

[2]Institut Jean Lamour (UMR CNRS 7198), University of Lorraine, B.P. 70239, 54506 Vandoeuvre-lès-Nancy, (FRANCE)

E-mail: Patrice.Berthod@univ-lorraine.fr

ABSTRACT

Plastic deformation or hardening leads to disorder in the crystalline structures of metals and alloys, and this deterioration may decrease their corrosion resistance. This concerns notably iron-based alloys, steels or cast irons. In this work it is wished to study such possible effect on simple binary carbon steels for carbon ranging from 0 to 1.6 wt.%C, in the simplest conditions: elaboration by casting, hardening by compression and corrosion in sulphuric solution, before exploring later more complex steels and cast irons, other modes of deformation and other aqueous solutions. In this first part these are the obtained microstructures, the hardness and compression properties which will be presented. A second part will be devoted to the corrosion behaviour and the influence of hardening of these electrochemical properties.

KEYWORDS

Cast carbon steels;
Carbon content;
Microstructure;
Hardness;
Compression properties.

INTRODUCTION

The plastic deformation or hardening of metallic alloy, during their shaping or their use, may significantly modify their microstructures[1]. One can easily characterize the microstructural consequences of plastic deformation by metallographic observations: structure initially equiaxed become in a new one presenting special orientations, phases geometrically changed, elongated grains... A lot of works have proved that plastic deformation may induce modifications of some alloy's properties, mechanical[2,3] or of other types such as the magnetic properties[4]. In the mechanical field the tensile, compression or shear strength, hardness may be modified, as for not-alloyed or highly alloyed steels, Cu alloys, Al alloys ... after cold-rolling or hot-rolling[5], extrusion[6] or plastic torsion deformation[7]. These properties may have lost their initial isotropic character, consequently to the orientated character of these deformations.

Some chemical properties may be also influenced by hardening, notably the corrosion behaviour. This is what was wished to be studied in this work.

For that a series of carbon steels were elaborated by casting. They were deformed by compression, then characterized in corrosion in their as-cast state and in the obtained hardened state. In this first part of the study this is the mechanical behaviours in compression of the steels which will be presented. The corrosion results will be presented in a second part.

EXPERIMENTAL

Elaboration of the alloys

A series of five carbon steels were elaborated by foundry. These Fe-xC alloys (x=0, 0.4, 0.8, 1.2 and 1.6 wt.%) were synthesized using a High Frequency induction furnace (CELES), by melting together pure iron and graphite. Each charge (total weight: about 40 g) was placed in the water-cooled crucible of the furnace, before being isolated from ambient air by a silica tube. In this chamber three cycles {7×10^{-2} mbar – vacuum; incorporation of 600 mbars of pure Argon} were applied, before finally establishing an internal atmosphere of 300 mbars of pure Ar). Melting and chemical homogenization of the liquid were achieved by respecting an isothermal stage of three minutes at 4 kilo Volts. By progressively decreasing the injected power the melt cooled and solidified to become a compact ingot.

Machining, metallography preparation and observations

The five obtained ingots were cut in order to obtain different types of samples. Two about {7 mm × 4 mm × 3 mm}-parallelepipeds were prepared from each of these ingots. One of the two parts was kept for metallographic characterization and the second one was devoted compression runs.

The parts destined for metallography investigations were initially embedded in a cold resin mixture (82% of CY230 resin and 18% of HY253 hardener, liquid products from ESCIL®), then ground with SiC papers from 120-grit up to 2400-grit. After intermediate ultrasonic cleaning these embedded samples were polished with textile disk enriched with 1µm hard particles in order to obtain a mirror-like surface.

After Nital etching (5 seconds of immersion in a {ethanol-4%HNO_3}, except for the ferritic one: 15 seconds), the metallography samples were observed using an optical microscope: Olympus, model BX51, equipped with a Toupcam camera driven by the Toupview software.

Indentation and compression runs

The hardness of the five steels was estimated by performing Vickers indentations under a 10kg-load. This was done three times per sample in order to obtain an average value and a standard deviation one.

The parallelepipeds especially prepared for the compression tests were plastically deformed using an Alliance RF/150 testing machine from MTS Systems. This one, equipped with a 150kN-cell for the force measurement, was driven by the Testworks4 software. The tests were continued until reaching a permanent deformation important enough to get a really hardened version of the same steels. The properties which were issue from these compression runs are the yield strength (transition from the elastic deformation to the plastic one) and the hardening parameters (k and n) involved in the Ludwig's equation (eq. 1):

$$\sigma = k \times \varepsilon^n \quad (1)$$

They can be easily deduced of the straight line resulting from the ln(σ) versus ln(ε) plotting since the logarithm of k is its ordinate at the origin while n is its slope (eq. 2).

$$\ln(\sigma) = \ln(k) + n \times \ln(\varepsilon) \quad (2)$$

RESULTS AND DISCUSSION

Microstructures, hardness and densities of the obtained steels

The as-cast microstructures of the obtained steels are illustrated in Figure 1 by optical micrographs taken after Nital etching.

The Fe-0.0C steel is clearly ferritic, with the grain boundaries revealed by the rather long (15 seconds) immersion in the Nital4 etchant. The Fe-0.4C steel is ferrite-pearlitic with well visible pearlite but also with a rather curious morphology of the ferrite grains (elongated/acicular, Widmanstätten

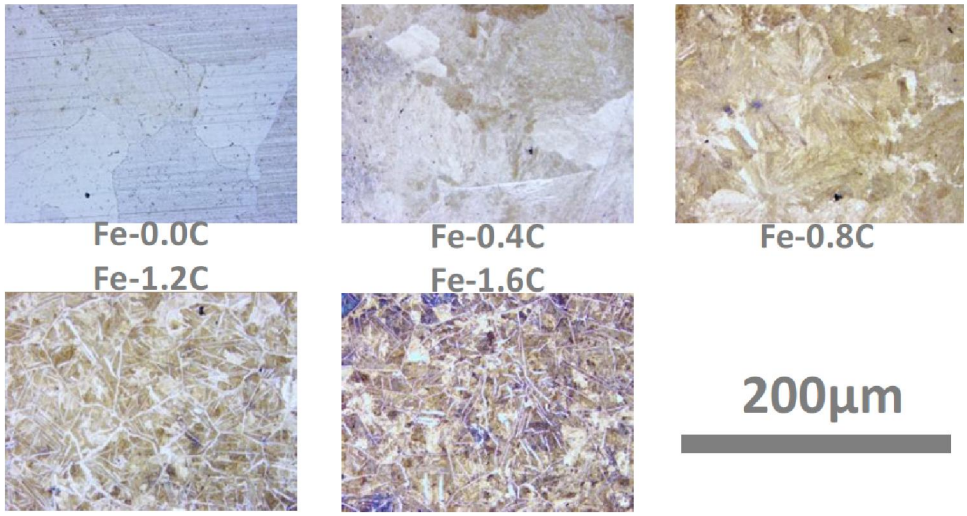

Figure 1 : The microstructures of the five steels (optical micrographs after nital etching)

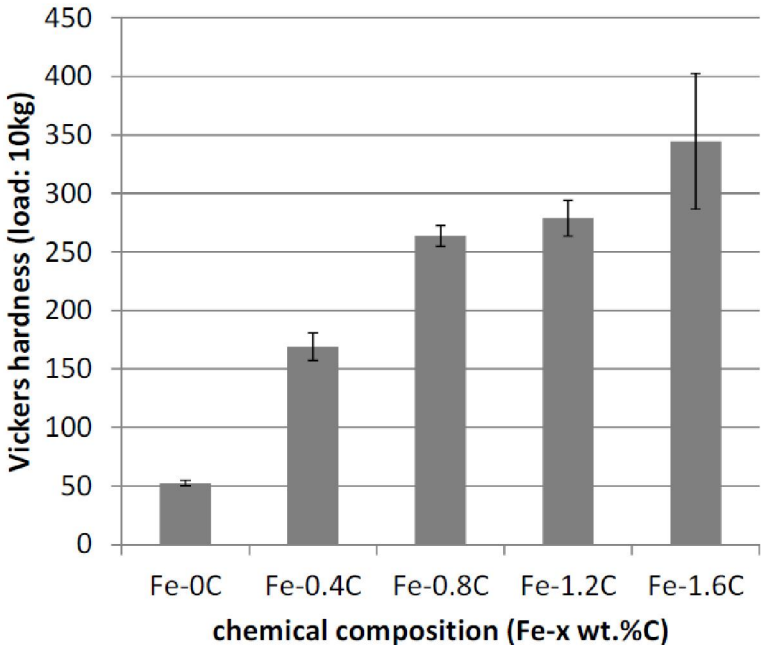

Figure 2 : 10-kg vickers hardness of the five steels, plotted versus the carbon content

shape). The Fe-0.8C steel is wholly pearlitic while the Fe-1.2C and Fe-1.6C steels are essentially pearlitic with also pre-eutectoid cementite (Fe_3C) present in the old austenitic grain boundaries but also seemingly crossing the pearlitic areas as Widmanstätten needles. The cementite surface fraction is logically higher in the 1.6C-containing steel than for the other hyper-eutectoid steel.

Thanks to this increasing fraction of cementite (very high hardness[8] compared to ferrite), eutectoid or pre-eutectoid + eutectoid, the hardness of the steels increases with the carbon content as usually observed with the carbon steels, as illustrated by Figure 2. Other physical property, one took advantage of the availability of the parallelepipeds for metallography and prepared for the compression tests, to use their measured dimensions and weight to estimate the volume mass of the five steels. As shown in Figure 3 one can see that the density remains globally constant (about 7.4-7.5), independently of the carbon content. The lack of accuracy of the dimensional measurement, notably due to a not perfectly regular shape of the parallelepipeds, leads to a rather broad error range, which remains however not sufficient to explain for example why the Fe-0.0C density is lower than the well-known value

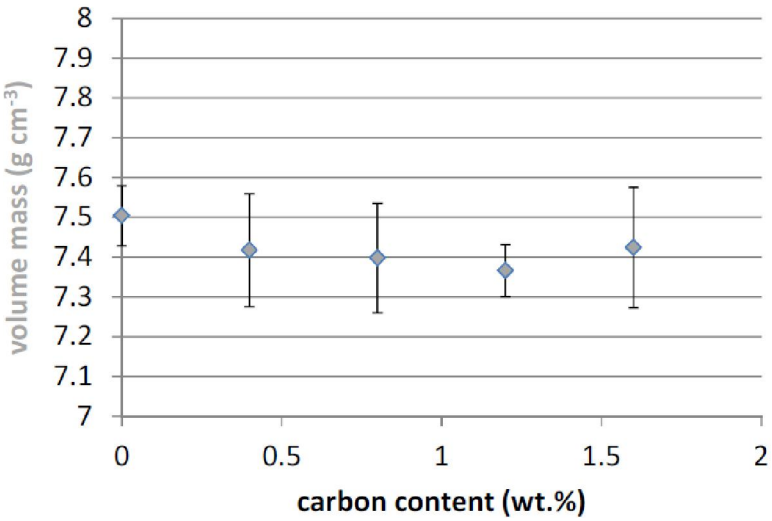

Figure 3 : 10-kg vickers hardness of the five steels, plotted versus the carbon content

TABLE 1: Values of the maximal stresses at which the compression stress were interrupted

Fe-x wt.% x=...	Maximal stress applied (MPa)
0	217
0.4	728
0.8	589
1.2	749
1.6	960

strains and maximal stresses, TABLE 1) led to the strain-stress curves plotted in Figure 4. The less resistant steel is unsurprisingly the ferritic Fe-0.0C one and the best one is the carbon-richest hypereutectoid steel. The curves obtained for the three other steels are logically intermediate but curiously rather close to one another. Since no extensometer was used this is the platen displacement were not accurately known and the smallest deformation are to be not considered (elastic deformations) and the apparent stiffness are logically scattered (elastic

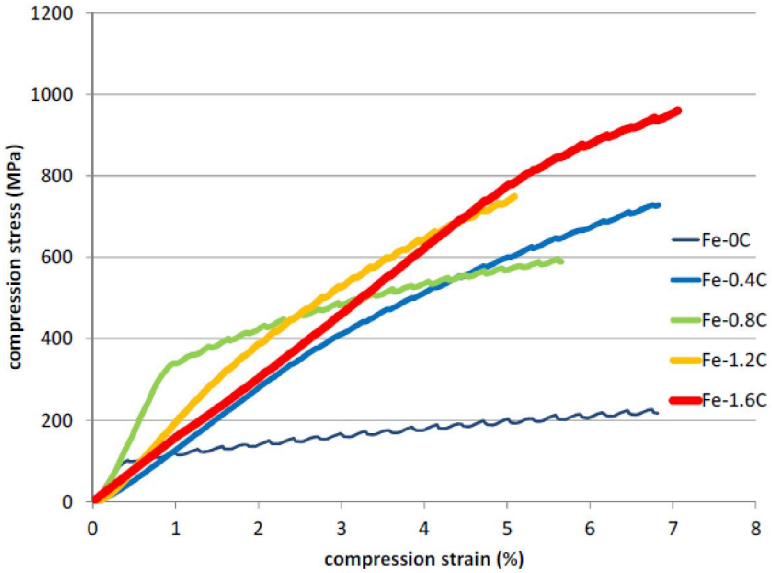

Figure 4 : The obtained compression curves

for pure Fe (pycnometric density of 7.86 g cm^{-3}[9]).

straight lines not comparable, Young's modulus not measurable). Only the greatest deformations (plastic deformation / hardening) may be really taken as

Behaviour in compression

The compression tests (interrupted after various

Full Paper

TABLE 2 : The yield strength versus the carbon content

Fe-x wt.% x=...	Yield strength (MPa)
0	101
0.4	278
0.8	286
1.2	293
1.6	681

accurate enough to be analysed. In contrast, the force being continuously accurately measured by the 150kN-cell, the stress can be also considered as accurate enough, despite the slight increase of the perpendicular section of the sample during the compression progress. One important property is the yield strength the value of which is the ordinate of the point of separation between the elastic straight line and the hardening concave curve. This point was more or less visible in the five curves strain-stress curves but its determination was attempted in all cases, this leading to the approximate values of yield strength displayed in TABLE 2. The lowest value was logically obtained for the ferritic alloy and the highest one for the carbon-richest hypereutectoid steel. If the values corresponding to the three steels with the medium carbon content values (0.4 to 1.2 wt.%) well increase with the carbon content they are very close to one another (around 285MPa, far from the 100MPa of the ferritic steel and the 700MPa of the carbon-richest alloy).

The plastic deformation parts of the compression curves were analyzed to extract the values of the hardening coefficients. The ln(σ) versus ln(ε) plots show that they globally well respect the Ludwig's law (Figure 5). The obtained values of the pre-exponential constant k and of the exponent n are given in TABLE 3. No clear relationship between the carbon content/cementite fraction and the k and n values obviously appears.

The compression runs were interrupted not at the same time for the five alloys (stresses which were applied at this moment given in TABLE 1). After test the permanent deformations, longitudinal (vertical, direction of force application, negative) and lateral (two horizontal deformations, positive), were measured and their values are given in TABLE 4. Even if this was not targeted the absolute value of the longitudinal deformation decreases when the carbon content of the steel increases (from -7% to -3% from 0 wt.%C to 1.6 wt.C). The new dimensions of the samples after compression were used again to value their densities. Their values are plotted together with the initial ones in Figure 6: it seems that the density generally tends increasing because of compression in the plastic domain.

General commentaries

The carbon carbon steels synthesized for this study, except the Fe-0.0C one, present microstructures which are not really classical for such very simple binary composition. Indeed, the ferrite grains in the ferrite-pearlitic steel are not blocky as usually found, but acicular, as needles grown from the old austenitic grain boundaries. The pre-eutectoid cementite also presents this Widmanstätten morphology in the hypereutectoid steels. This may be due to the fast solid state cooling following the rapid solidification, in contact with the water-cooled copper crucible of the high frequency induction furnace. Maybe these steels merited post-foundry austenitization heat-treatment finished by a slower cooling. The hardness issued from Vickers macro-indentation nevertheless remain globally conform to the values commonly observed for carbon steels of the same compositions. The compression tests carried out to bring these steels a hardened state showed that these ones present various levels of mechanical properties, more or less logical (e.g. yield strength)

TABLE 3: The {ln(σ)=f[ln(ε)]}-plot of the plastic deformation part of the compression curves and the obtained values of the hardening constants k and n involved in the Ludwig's equation

Hardening constants ($\sigma = k \times \varepsilon^n$)	k (MPa)	n
Fe-0.0C	422	0.252
Fe-0.4C	1902	0.329
Fe-0.8C	1054	0.200
Fe-1.2C	1988	0.309
Fe-1.6C	1350	0.105

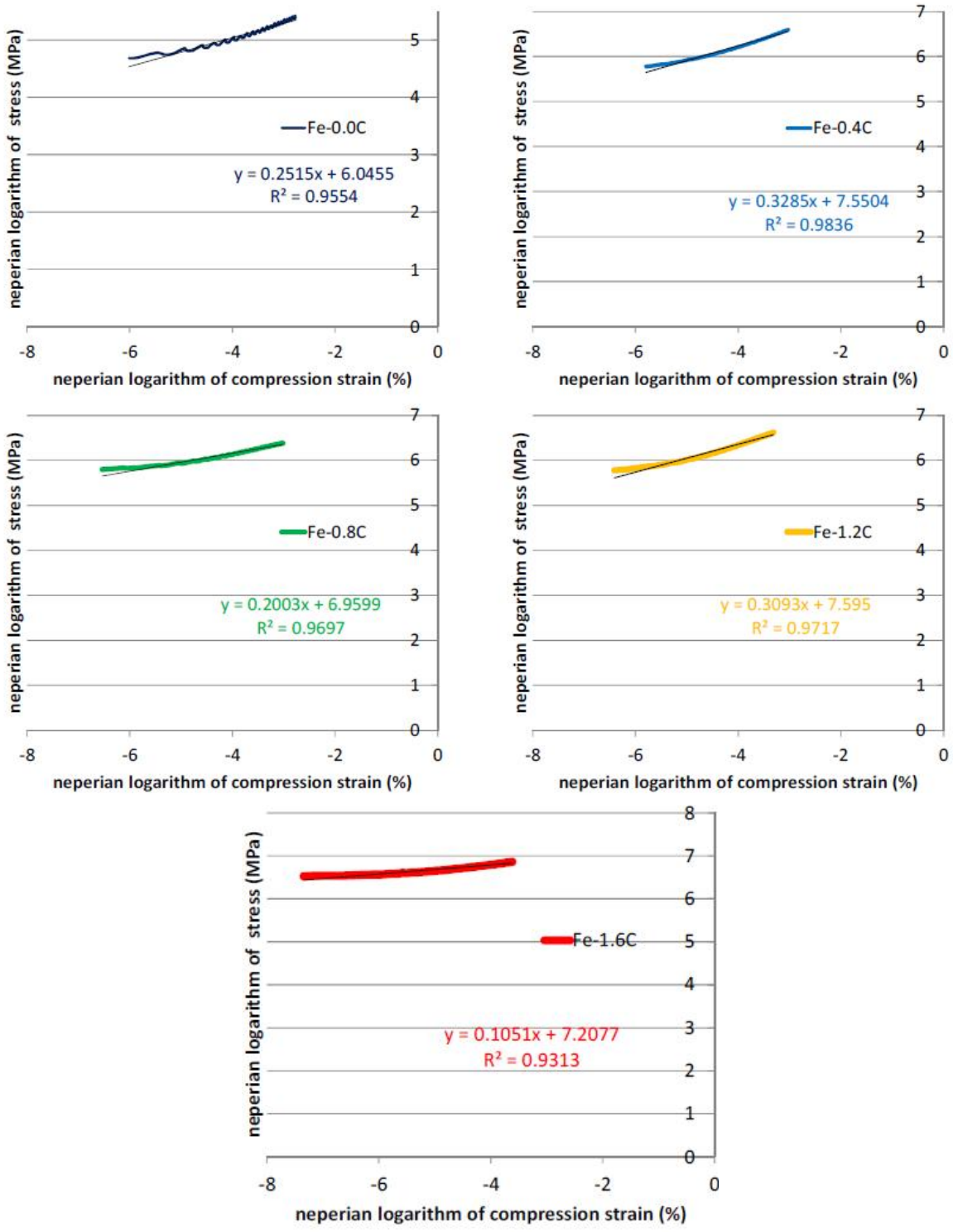

Figure 5 : The {ln(σ)=f[ln(ε)]}-plot of the plastic deformation part of the compression curves and the obtained values of the hardening constants k and n involved in the Ludwig's equation

or very scattered without relationship with the carbon content then the cementite fraction (e.g. hardening parameters k and n). Because of strength difference issued from the different carbon content it was not possible to achieve the same permanent deformation for the five samples, the stiffest carbon-rich steels being less plastically deformed than the low carbon ones. This will be to be taken into account when the electrochemical measurements devoted to characterize their behaviors in corrosion will be

Full Paper

TABLE 4 : The permanent deformations obtained longitudinally and laterally

Alloy	Relative longitudinal deformation (ε_{xx})	Relative Lateral deformations (ε_{yy} and ε_{zz})
Fe-0.0wt%C	-7.10%	+2.41% and +1.76%
Fe-0.4wt%C	-4.47%	+4.70% and +1.57%
Fe-0.8wt%C	-5.56%	+1.97% and +1.37%
Fe-1.2wt%C	-3.18%	+0.87% and +1.73%
Fe-1.6wt%C	-3.06%	+0.46% and +0.63%

Density versus the deformed state)

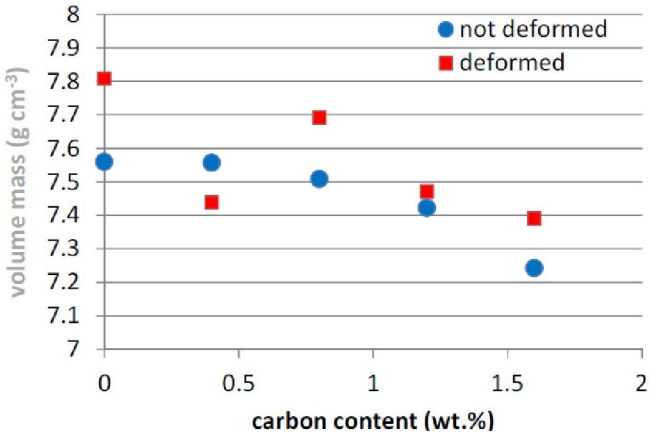

Figure 6 : Evolution of the volume mass of the five steels with the carbon content and with the deformed state

carried out[10].

CONCLUSIONS

After the elaboration of the five binary steels with increasing contents in carbon and the hardening of samples issued from the obtained ingots, the present work will be carried on to characterize the effect of the hardening on the corrosion behaviour of these five nuances of carbon steel. The rate of permanent deformation which was not the same for all steels will not allow the comparison between deformed steels with different carbon content. But the comparisons between steels in their as-cast states will be possible.

ACKNOWLEDGMENTS

The authors thank Mathieu Lierre for the preparation of the solution as well as for its assistance.

REFERENCES

[1] J.M.Dorlot, J.P.Baïlon, J.Masounave; "Des Matériaux", Editions de l'Ecole Polytechnique de Montréal, Montréal **(1986)**.
[2] Y.D.Koryagin, N.T.Kareva, M.A.Smirnov; Physics of Metals and Metallography, **55**, 187 **(1983)**.
[3] V.G.Serebryakpv, E.I.Ehstrin; Fizika Metallov I Metallovedenie, **2**, 130 **(1992)**.
[4] A.H.Qureshi, L.N.Chaudhary; Journal of Applied Physics, **41**, 1042 **(1970)**.
[5] E.L.Svistunova, A.A.Gulyaev, A.B.Oralbaev; Fizika Metallov I Metallovedenie, **78**, 108 **(1994)**.
[6] J.Zdunek, P.Widlicki, H.Garbacz, J.Mizera, K.J.Kurzydlowski; Diffusion and defect data pt.B: Solid State Phenomena, **114**, 171 **(2006)**.
[7] A.V.Korzinkov, Y.V.Ivanisenko, D.V.Laptionok, I.M.Safarov, V.P.Pilyugin, R.Z.Valiev; Nanostructured Materials, **4**, 159 **(1994)**.
[8] M.Umemoto, Y.Todaka, K.Tsuchyia; Materials Science Forum, **426-432**, 859 **(2003)**.
[9] P.T.B.Shaffer; High-temperature materials, N°1: Materials Index, Plenum Press, New York, **(1964)**.
[10] M.Belhabib, P.Berthod; Materials Science: An Indian Journal, *to be submitted.*